[1]

Characterization of Long-Term Stability of Suomi NPP Cross-Track Infrared Sounder (CrIS) Spectral Calibration

Yong Chen, Yong Han, and Fuzhong Weng

***Abstract*— Since early 2012, the Cross-track Infrared Sounder (CrIS) on board the Suomi National Polar-Orbiting Partnership (S-NPP) Satellite has continually provided the hyperspectral infrared observations for profiling atmospheric temperature, moisture and greenhouse gases. The CrIS radiance data are also directly assimilated into global numerical weather prediction (NWP) models to improve the medium-range forecasts. These important applications require accurate CrIS calibration. Since CrIS radiometric accuracy depends on the accurate spectral calibration, it is important to reduce the spectral uncertainty and increase the calibration stability for weather and climate applications. In this study, the accuracy of CrIS spectral calibration and its stability are assessed using the operational Sensor Data Record (SDR) data generated by the Interface Data Processing Segment (IDPS). A spectral validation method is developed and applied to clear scene data over ocean from September 22, 2012 to April 19, 2016. It is shown that CrIS metrology laser wavelength varies within 3 ppm (parts per million) as measured by the Neon calibration subsystem. While the current CrIS operational algorithm is designed to have a spectra error less than 2 ppm, the actual spectral errors are about 4 ppm due to the IDPS software bugs. A new correction method is applied to fix the bugs and to further improve CrIS spectral calibration. It is found that the CrIS spectral calibration accuracy is less than 1 ppm in both normal and full spectral resolution SDR data sets.**

***Index Terms*— CrIS, Spectral accuracy, Long-Term spectral stability, Neon calibration subsystem, Suomi NPP, Spectral validation method**

I. Introduction

The Cross-Track Infrared Sounder (CrIS) is a Fourier transform spectrometer on board the Suomi National Polar-Orbiting Partnership (S-NPP) satellite, which was launched on October 28, 2011. Since April 19, 2012, the Joint Polar Satellite System (JPSS) ground processing system called the Interface Data Processing Segment (IDPS) has continuously generated the CrIS Sensor Data Record (SDR) and delivered to user communities. For each scan, CrIS collects 30 fields of regard (FORs) Earth scene data. Each FOR includes nine fields of view (FOVs) which are arranged in a 3×3 array of detectors. At each FOV, CrIS measures the infrared radiance covering three spectral bands. It provides a total of 1305 radiance channels in the normal spectral resolution (NSR) operational mode for sounding the atmosphere. The NSR resolutions are 0.625, 1.25, 2.5 cm^{-1} for the long-wave (LW), mid-wave (MW), and short-wave (SW) bands, respectively. CrIS can also be operated in a full spectral resolution (FSR) mode, at which the MW and SW band interferograms are recorded with the same maximum path difference (MPD) as that at the LW band. The spectral resolution for all three bands at FSR is 0.625 cm^{-1} and thus the FSR data has a total of 2211 channels. Details for CrIS channels and their characteristics are summarized in Table I.

Currently, there are four hyperspectral infrared sounders on-board operational and research satellites. In addition to CrIS on board the S-NPP satellite, the Infrared Atmospheric Sounding Interferometer (IASI) flied on the EUMETSAT Meteorological Operational Satellite (MetOp) platforms from 2006 (including MetOp-A and B), and the Atmospheric Infrared Sounder (AIRS) on the NASA Earth Observing System (EOS) Aqua platform from 2002. AIRS is a grating spectrometer, while CrIS and IASI are the Michelson interferometers. These instruments provide a high-vertical resolution of temperature and water vapor information critically important for improving numerical weather prediction (NWP) assimilation and forecast results [1-3], supply extensive information about trace gases, cloud properties, and surface properties for climate applications [2, 4, 5], and can be used as space reference sensors to calibrate and validate other IR sounders [6-8]. All these applications require the hyperspectral infrared radiances with high and stable calibration accuracy.

CrIS high calibration accuracy is achieved through its excellent instrument design, well-conducted pre-launch calibration, and intensive post-launch validation. The CrIS overall performance in spectral, radiometric, geometric calibrations and noise performance can be found in the

[1]Manuscript received June 2016; revised September 2016; accepted October 2016. This study was supported by NOAA grant NA14NES4320003 (Cooperative Institute for Climate and Satellites-CICS: Cooperative Agreement 2014-2019) at the University of Maryland/ESSIC. The contents of this paper are solely the opinions of the authors and do not constitute a statement of policy, decision, or position on behalf of NOAA or the U. S. Government.

Y. Chen is with Earth System Science Interdisciplinary Research Center, University of Maryland at College Park, College Park, MD 20740 USA (e-mail: Yong.Chen@noaa.gov).

Y. Han and F. Weng are with the Center for Satellite Applications and Research, National Environmental Satellite, Data, and Information Service (NESDIS), National Oceanic and Atmospheric Administration, College Park, 20740, USA (e-mail: Yong.Han@noaa.gov; Fuzhong.Weng@noaa.gov).

TABLE I
CRIS NSR MODE AND FSR MODE SDR SPECTRAL CHARACTERISTICS

Instrument	Frequency Band	Spectral Range (cm^{-1})	Number of In-band Channel (Unapodized Channel)	Spectral Resolution (cm^{-1})	Effective Max. Path Difference (MPD) (cm)	Number of channels with Guard Bands (N_b)	Decimation Factor (DF_b)
CrIS	LW	650 to 1095	713* (717)	0.625	0.8	864	24
	MW	1210 to 1750	433* (437)	1.25	0.4	528	20
	SW	2155 to 2550	159* (163)	2.5	0.2	200	26
CrIS_FSR	LW	650 to 1095	713* (717)	0.625	0.8	864	24
	MW	1210 to 1750	865* (869)	0.625	0.8	1050	20
	SW	2155 to 2550	633* (637)	0.625	0.8	797	26

*Apodized channel

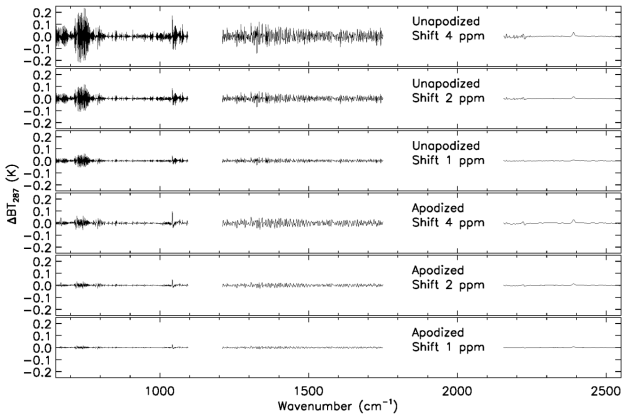

Fig. 1. Impact of spectral accuracy on radiometric accuracy in terms of brightness temperature difference for a typical warm scene with respect to an effective BT of 287 K for three different spectral shifts (1 ppm, 2 ppm, and 4 ppm) at CrIS three bands for both unapodized and apodized spectra.

previous studies [9-13]. Those previous studies demonstrated that the CrIS SDR data meet calibration requirements, thus making it an exceptional asset for weather applications. The CrIS SDR data will be further improved for climate applications with its fine-tuning of calibration coefficients in NOAA reprocessing project.

The CrIS radiometric accuracy depends on the accurate spectral calibration. Quantifying the impact of CrIS spectral accuracy in term of radiance or brightness temperature (BT) is very important to understand CrIS observation uncertainty, and to correctly use these observations in the satellite data assimilation systems that lead to improve weather forecasting and in the climate systems to derive the climate trend. Figure 1 shows the CrIS brightness temperature errors due to three spectral shifts (1 ppm, 2 ppm, and 4 ppm) in the spectral calibration, for both unapodized and Hamming-apodized radiances (numerical weather predication assimilation centers to date only use CrIS apodized radiances) for a typical warm scene with respect to an effective BT of 287 K (Internal Calibration Target nominal temperature). For a given spectral shift, the BT impact is much larger from unapodized spectra than apodized one. For example, when spectral shift is 4 ppm, the BT difference for the unapodized spectra can be as large as 0.25 K at spectral range [710 cm^{-1}, 770 cm^{-1}], a very critical region to derive temperature profile, while the difference for the apodized spectra is small (~0.03 K) at that range. This figure indicates that a 1 ppm spectral calibration error as shown in relative FOV-2-FOV spectral calibration differences (see Table II), for a Hamming-apodization, should limit the BT impact to about 0.02 K, which should be small enough for successful NWP bias correction. Although the absolute BT difference may be scene dependent, the impacts are on the same order for all the representative Earth scenes. In this study, we mainly focus on the spectral validation methods and select those sensitive spectral ranges to evaluate CrIS spectral accuracy and stability using the long-term CrIS SDR data. Two basic spectral validation methods [11, 14] have been developed: 1) Relative spectral validation, which uses two uniform observations to determine the frequency offsets relative to each other; and 2) Absolute spectral validation, which requires an accurate forward radiative transfer (RT) model to simulate the top of atmosphere radiance under clear conditions and correlates the simulation with the observed radiance until a maximum correlation is found.

The results of the study provide assessment of the accuracy and long-term stability of the CrIS spectral calibration during the S-NPP mission life time. A new method different from the operational processing software is proposed to improve the CrIS spectral stability for the reprocessed NSR and offline FSR CrIS data. Section II describes the CrIS spectral calibration system. Section III presents the cross-correlation method and the cloud detection algorithm using the forward model simulated radiances. Section IV focuses on the selection of the spectral region to determine the spectral error. The CrIS operational SDR data long-term spectral accuracy and stability are discussed in section V. A summary is presented in section VI.

II. CRIS SPECTRAL CALIBRTION SYSTEM

As mentioned above, each CrIS FOR includes nine FOVs arranged in a 3×3 array of detectors. The interferometer axis is designed and pointed to the center of FOV 5. All nine detectors receive the radiation incident from the off-axis and thus require a correction of the instrument self-apodization (SA) effect. The CrIS spectral calibration accuracy can be compromised by the inaccurate geometry of the focal plane detectors that determines the exact alignment of the detectors to the interferometer boresight axis. Since FOV 5 in CrIS is nominally centered in the interferometer axis, it is largely

immune to the focal plane position uncertainties. The geometry of the focal plane detectors is very static once CrIS is stabilized in-orbit [11, 15]. The spectral calibration can also be impacted by the inaccurate knowledge of the metrology laser wavelength that determines the interferogram optical path difference (OPD) sampling positions. To determine the metrology laser wavelength which may vary with time, CrIS is designed with a Neon calibration subsystem which is not available for IASI. Radiation is emitted at 703.45 nm from a low-pressure Neon lamp co-aligned with the interferometer axis and is used as a spectral calibration reference. During a sweep of a single interferogram, fringe counts (including fractional fringes) from both the Neon lamp and the metrology laser are measured. Since the sweep contains a fix number of metrology laser fringes, the metrology laser wavelength can be measured by using the Neon emission wavelength and the interpolated fractional Neon fringe count at the beginning and end of the OPD sweep using a high-speed clock. The Neon lamp is activated for 10 seconds once every 109 minutes, and the measurements are stored in the CrIS engineering data packet so that the precise metrology laser wavelength can be computed for use in SDR processing. A calibration interval of 109 minutes instead of the 101 minutes orbit period is chosen to spread out the dependence of the Neon emission measurement on the orbital position over a long-time data record. Therefore, the metrology laser calibration process can be characterized and tracked for any orbital variation.

The CrIS detector focal plane geometry and the Neon lamp effective wavelength are initially determined during thermal vacuum (TVAC) testing by recording the transmittance spectra of CO_2, CH_4, and HBr, which have strong spectral features in bands 1, 2, and 3, respectively. The determination processes are thoroughly documented in Strow, et al. [11]. The prelaunch values derived from TVAC data for the focal plane position of each FOV (including FOV size and offset angles, referred to as instrument line shape (ILS)) and then adjusted with the intensive post-launch validation, as well as the Neon wavelength are inserted into the CrIS Engineering Package (EP), which is used by the SDR software to transform the raw measurements to calibrated radiance spectra.

The operational CrIS SDR algorithms are implemented into two software packages, which share the same processing code. One is for the operational IDPS package. The other is for the Algorithm Development Library (ADL), an off-line version of the IDPS to develop and improve new algorithms, fix bugs, and investigate anomalies. The spectral calibration is an essential component in the calibration algorithms, and includes three operations: post filter matrix, resampling matrix, and SA correction matrix. The post filter suppresses the noise signal in the guard bands that results from the radiometric calibration, which has no impact on the CrIS spectral characterization. The resampling matrix performs two functions: changing the spectral resolution to the required resolution, and interpolating the spectrum from the sensor wavenumber grid onto the user-defined wavenumber grid. For CrIS spectra, the spectra grid or the spectral distance between two adjacent channels is equal to the spectral resolution. The raw spectral resolution on sensor grid for a given band, *b,* is defined as

$$\Delta\sigma_b = 1/\left(N_b * DF_b * \lambda_s\right), \tag{1}$$

where N_b is the number of interferogram samples after decimation, and DF_b is the decimation factor. λ_s is the sampling interval of the interferogram, referred as resampling wavelength, and is equal to half of the metrology laser wavelength. The metrology laser wavelength varies slowly with time which is highly correlated with the interferometer baseplate temperatures [11], resulting in the variation of the spectral resolution and grid size of the raw spectra. Let $\delta\lambda$ represent the change of the sampling interval from λ_s to λ_s':

$$\lambda_s' = \lambda_s + \delta\lambda \,. \tag{2}$$

The spectral resolution as well as the spectral spacing is then changed to $\Delta\sigma_b'$ from $\Delta\sigma_b$ as

$$\Delta\sigma_b' = 1/\left(N_b * DF_b * \lambda_s'\right) \,. \tag{3}$$

The relative frequency or spectral error in channel n (referred as sampling error) due to the metrology laser wavelength drifts therefore can be derived as:

$$\Delta\nu_s(\text{ppm}) = \frac{\left(\sigma_{b,n} - \sigma_{b,n}'\right) * 10^6}{\sigma_{b,n}} = \frac{\delta\lambda * 10^6}{\lambda_s + \delta\lambda} \approx \frac{\delta\lambda * 10^6}{\lambda_s} \,. \tag{4}$$

The relative spectral error is independent of the wavenumber σ. Since the peak-to-peak variation of the S-NPP metrology laser wavelength is about 3 ppm (10^{-4} %) per year (see Fig. 2), the approximation in (4) is valid. The resampling matrix maps the spectra from the sensor grid to the user grid and therefore the amount of relative spectral error occurring in the raw spectra is the same as that in the user grid after spectral resampling. In order to take the laser wavelength variation into account, the resampling matrix needs to be frequently updated to reflect the changes in sensor spectral grid. While the CrIS spectral calibration system measures the laser wavelength periodically roughly once per orbit, the current spectral calibration algorithm does not update the resampling matrix as often as the Neon measurements.

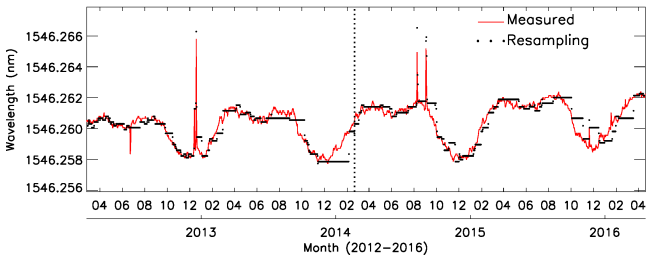

Fig. 2. Daily averaged metrology laser wavelength (red line) and resampling wavelength (black dot) recorded in the NOAA IDPS SDRs data. The vertical dashed line indicates the IDPS software updated to the version MX 8.2 on February 20, 2014 (see text). Note that the black lines are formed by the black dots which overlap each other due to the high time resolution.

The SA correction matrix corrects the spectral distortion due to radiance beam divergence effect from the spectra. At CrIS channel, spectral response functions (SRF) is an ideal Sinc function. Although the SA correction matrix is a function of wavenumber, simulations show that it is not sensitive to the resampling wavelength change if the laser wavelength variation is small (less than 100 ppm). As mentioned earlier, the geometry of the focal plane detectors does not change significantly over time. Therefore the SA correction matrix does not need update possibly for the whole mission of the instrument. In CrIS SDR processing, the three matrices operating for post filter, resampling, and SA correction are combined into a single matrix, referred as Correction Matrix Operator (CMO).

The computational expense of the SA correction matrix is very costly. Thus, in the operational design, the CMO is rebuilt only under two following conditions: 1) The cumulative variation of the metrology wavelength exceeds 2 ppm to the initial metrology laser wavelength (2*resampling wavelength, which is saved in the SDR processing). 2) The ILS parameters are updated in the Engineering Packet. A CMO file can be operationally provided at the initialization of the SDR process, and if it is not available at that point, a new CMO will be computed using the calibration parameters in EP from the input Raw Data Record (RDR) data stream which is available every 4 minutes. During the S-NPP mission, the EP has been updated several times from version 31 to 36. Among them, only two updates are related to the change of the ILS parameters for the calibration refinements, version 33 (April 11, 2012) and version 36 (February 20, 2014). These update significantly improved the spectral and radiometric calibration absolute accuracies and relative agreement among the nine FOVs [9, 11]. When a new CMO is generated, the resampling wavelength is equal to half of the new value of the metrology laser. At that point, there should be no sampling spectral error occurring, assuming the Neon measurement of the metrology laser wavelength is perfect. Since the resampling wavelength keeps the same when the cumulative variation of the metrology laser wavelength is less than 2 ppm, the sampling spectral error due to the drift of the metrology laser wavelength can be easily obtained. Unfortunately, due to an IDPS software bug, the resampling wavelength used to compute the resampling matrix is saved incorrectly in the official CrIS SDR data, which makes it impossible to know the exact metrology wavelength used to produce the observed CrIS radiance spectra. This bug is seemingly fixed on November 14, 2013 when the IDPS software was updated and the resampling wavelength for CMO calculation was archived in the CMO file. However, the resampling wavelength is still not correct on some occasions, and changes very frequently even when the cumulative variation of the metrology laser wavelength is less than 2 ppm. This can be clearly seen in Fig. 2. It shows the daily averaged metrology laser wavelength (red line) and resampling wavelength (black dot) recorded in the IDPS SDR data over four years period from February 25, 2012 to April 19, 2016. The metrology laser wavelength changes over time with peak-to-peak variation less than 3 ppm. It also shows yearly periodical variation, primarily due to the temperature changes in the interferometer baseplate. These sharp spikes with large metrology laser wavelength change (much larger than 2 ppm) on December 19, 2012, August 9, 2014, and September 2, 2014 are due to S-NPP spacecraft issues with instrument on safe mode, not CrIS malfunctions. The vertical dashed line in this figure indicates the IDPS software updates as well as EP version of 36 uploaded in RDR data stream on February 20, 2014. An error in the correction matrix computation for FOV 5 is fixed in the software, and new ILS parameters and non-linearity coefficients are also updated in EP version 36. These updates result in 1.4 ppm and 2.2 ppm spectral shift for band 1 and band 2 for FOV 5 before and after updates [11], but impacts for other FOVs are small and can be negligible spectrally.

Due to the IDPS software bugs and refinements of calibration coefficients, it is impossible to use the relative spectral shift of resampling wavelength and metrology laser wavelength to evaluate the CrIS spectral accuracy and stability during the CrIS mission. It becomes very necessary to use the absolute spectral validation method to assess the CrIS long-term spectral characterization.

III. SPECTRAL VALIDATION USING CROSS-CORRELATION METHOD

A. Cross-correlation Method

Assuming two spectra S_1 and S_2 having the same data length and resolution, each spectrum is a function of wavenumber σ. The correlation coefficient and standard deviation between the two spectra are adapted from [14]

$$r_{S_1S_2} = \frac{\sum_{i=1}^{n}(S_{1,i}-\overline{S_1})(S_{2,i}-\overline{S_2})}{(n-1)D_{S_1}D_{S_2}} = \frac{\sum_{i=1}^{n}(S_{1,i}-\overline{S_1})(S_{2,i}-\overline{S_2})}{\sqrt{\sum_{i=1}^{n}(S_{1,i}-\overline{S_1})^2(S_{2,i}-\overline{S_2})^2}}, \tag{5}$$

$$D_{S_1S_2} = \sqrt{\sum_{i=1}^{n}[(S_{1,i}-\overline{S_1})-(S_{2,i}-\overline{S_2})]^2 \Big/ (n-1)}. \tag{6}$$

where n is the number of channels, $\overline{S}$ and D are the mean and standard deviation of spectrum S, respectively. Since the effect of CrIS frequency calibration error (SA correction error and sampling error) is stretching (or shrinking) the original spectrum along the frequency domain, a shift factor or offset α is defined so that $\sigma' = \sigma(1+\alpha)$. A series of spectra $S_2(\sigma')$ from the original one $S_2(\sigma)$ could be obtained by

varying the shift factor within a range $[\alpha_1, \alpha_2]$. The frequency offset that produces the maximum correlation coefficient $r_{S_1(\sigma)S_2(\sigma')}$ or minimum standard deviation $D_{S_1(\sigma)S_2(\sigma')}$ is the frequency error between these two spectra $S_1(\sigma)$ and $S_2(\sigma)$. Our sensitivity study shows that the shift factor can be efficiently identified by both quantities computed with (5) and (6) if the two spectra are from clear uniform observation/simulation. It also indicates that the absolute radiance difference between the two spectra is not sensitive to the frequency offset and is thus not a determining factor. In this study, we use the maximum correlation coefficient to detect the frequency offset.

The scheme to detect the frequency offset from CrIS observation using the relative method and absolute method is summarized in the following steps.

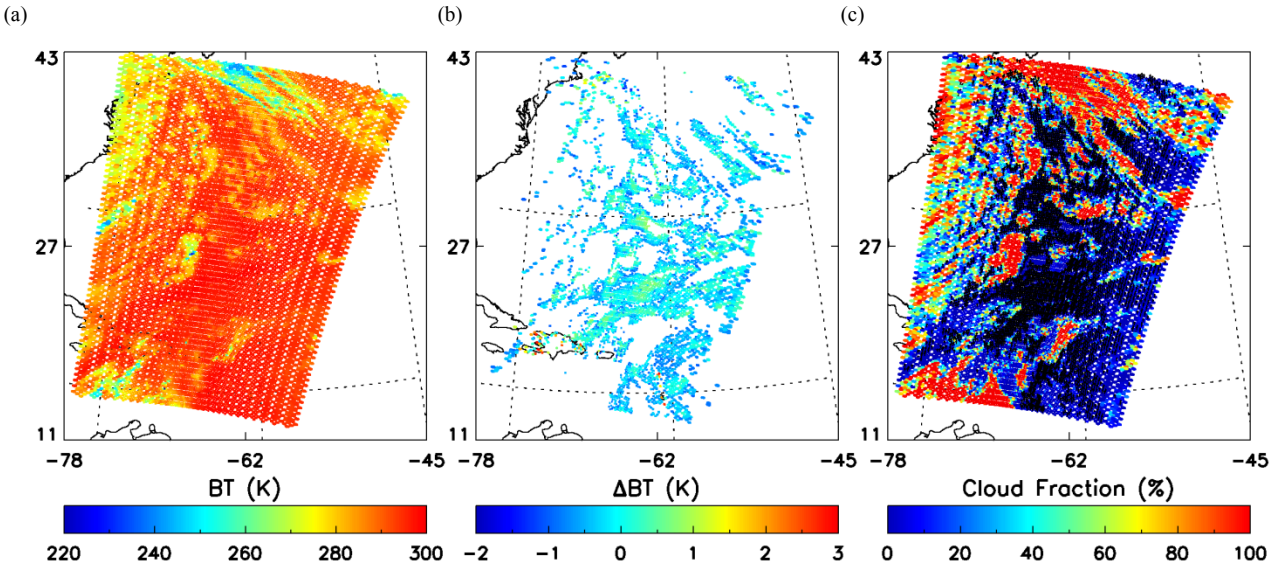

Fig. 3. Testing of CrIS Cloud detection algorithm for window channel 401 at 900.0 cm^{-1} on October 30 2012 over Atlantic Ocean. (a). CrIS observed BTs; (b) Observation minus CRTM simulation over clear sky using CrIS hyper-spectral cloud detection algorithm; (c) Cloud fraction determined from the collocated VIIRS (the black dots indicated the clear sky from (b)).

1) A pair of clear CrIS unapodized spectra is chosen. For the relative method, both spectra are from observations, while for the absolute method, one is from observation, and the other is from forward model simulation (clear scene detection and forward model simulation will be discussed at section III.B).
2) The spectra are interpolated on finer spectral grid using Fast Fourier Transform (FFT) method. Specifically, these spectra are first transformed by FFT to the interferogram space, and the maximum path difference (MPD) is increased by padding zeros in the interferogram space. The pair of the fine grid spectra are then obtained by the inverse FFT on the interferograms.
3) The cross-correlation method is applied to the pair fine grid spectra to finally get the maximum correlation coefficient and minimum standard deviation by shifting one of the spectra in a given shift factor ranging [-6 ppm, 6 ppm] with step size 0.1 ppm.

B. Cloud Detection and Forward Simulation of Hyper-spectral Radiance

To use the cross-correlation method to determine the frequency offset of two spectra, it is very important that these two spectra are spatially uniform and over a clear scene. The effects of possible contamination by clouds or spatially varying humidity in the CrIS observations are detected by using the hyper-spectral IR cloud detection algorithm [16] coupled with Community Radiative Transfer Model (CRTM)) [17-19]. We defined an overcast variable which contains overcast radiance profile assuming the presence of a black cloud at each CRTM level. The cloud sensitive height for a particular channel is assigned by finding the level where the difference between the simulated overcast and clear radiance is less than 1%.

$$\frac{\left|R_{clear} - R_{cloudy}\right|}{R_{clear}} < 0.01 \quad (7)$$

where R_{clear} is the simulated clear sky radiance, and R_{cloudy} is the overcast radiance. Based on (7), the cloud sensitive height should not be higher than the weighting function peaking height due to the fact that the definition of the cloud sensitive height at the level where the energy contribution of black cloud should not exceed 1% of the clear radiance. The cloud detection algorithm is worked as followings based on the differences between observations and simulations: 1) the channels are first ordered according to their cloud sensitivity height: the highest channel goes first and the lowest channel last; 2) the resulting ranked brightness temperature departures

from observation are smoothed with a moving-average filter in order to reduce the effect of instrument noise; 3) the clear channels are detected by searching the level in which a cloud no longer significantly affects the radiances and the BT departure and local gradient fall below the pre-determined thresholds; 4) all channels below this point are marked as cloudy and all channels above as clear. The accuracy of this algorithm is dependent on the accuracy of the forward model and its input atmospheric profiles and surface conditions. To make sure the simulated radiances having high accuracy, we use the atmospheric profiles (pressure, temperature, water vapor, and ozone) from European Center for Medium-range Weather Forecasts (ECMWF) 3-hour analysis/forecast model data. The CrIS radiances are simulated using the nearest matching ECMWF operational forecast model profiles through the spatial and temporal interpolation. The four forecast grid points surrounding the satellite pixel are bilinearly interpolated to the location of satellite pixel location, then a linear temporal interpolation in time is performed using the two forecast fields that bound the CrIS observational time.

To validate the cloud detection algorithm, we have compared the results with coincident cloud mask products from Visible Infrared Imaging Radiometer Suite (VIIRS) [20], an imaging instrument onboard the same satellite as CrIS. VIIRS has very high spatial resolutions (375m at nadir for its Imaging Bands) compared with CrIS nadir spatial resolution of 14 km. Figure 3 shows the distribution of data flagged clear from CrIS cloud detection overlaid upon a coincident and collocated cloud mask from VIIRS over the Atlantic ocean on October 30, 2012 after the Superstorm Sandy hit New York City. Figure 3a shows an image from CrIS channel 401 at 900 cm^{-1}. This is one of the CrIS window channels which have weighting function peaking height and cloud sensitive height at/near surface. When clouds are present, the brightness temperatures from this channel will normally decrease compared with those from clear sky. The lower brightness temperatures below 280 K may indicate the cloud presence. Figure 3b shows the cloud-free BT differences between CrIS observation and CRTM simulations at this window channel. The cloud-free areas are determined by using CrIS hyper-spectral cloud detection algorithm. The absolution differences for the majority of these pixels are less than 1 K over ocean. Some pixels over land have larger differences (~3 K) which suggest that the land surface skin temperature may not be accurate enough. Figure 3c shows the cloud fraction from the collocated VIIRS at CrIS Field of view. Cloud-free areas from 3b are indicated by the black dots in Fig. 3c. There is a remarkable correspondence between areas that clear (low cloud fraction) from VIIRS and places where CrIS channel 401 are determined clear, indicating that most CrIS channels have been flagged clear since the rank of cloud sensitivity from this channel is very low. However, it is evident that there are some areas where it appears from the VIIRS that the scene is clear or most clear (cloud fraction less than 20%), but CrIS channel 401 has been flagged cloudy. The comparison result between CrIS and VIIRS cloud detection shows that CrIS cloud detection algorithm works very well and is conservative at detecting clear sky. Due to the large errors in modeling land surface skin temperature and emissivity, we only consider the results over ocean in this study hereafter.

The absolute cross-correlation method is quite sensitive to the errors in the computed spectra especially related to the spectral resolution. Since CRTM simulated radiances are apodized with Hamming function which performs a three-channel smooth filter in the spectral domain, the width of channel spectral response function (SRF) is increased by 50.4% compared to that from the original ideal sinc function. We use a more accurate forward model LBLRTM version 12.2 [21] to simulate these detected CrIS clear scenes over ocean and perform absolute spectral accuracy validation. In order to perform the relative spectral validation among CrIS nine FOVs and the absolute spectral validation, and avoid the Doppler shifts due to the rotation of the Earth [14] and solar reflection contribution at daytime [19], only night time clear ocean scenes for all nine FOVs at nadir FORs (15th and 16th) are chosen from these detected clear scenes. The corresponding matched ECMWF fields as well as model default CH_4 and CO profiles are used as inputs into the

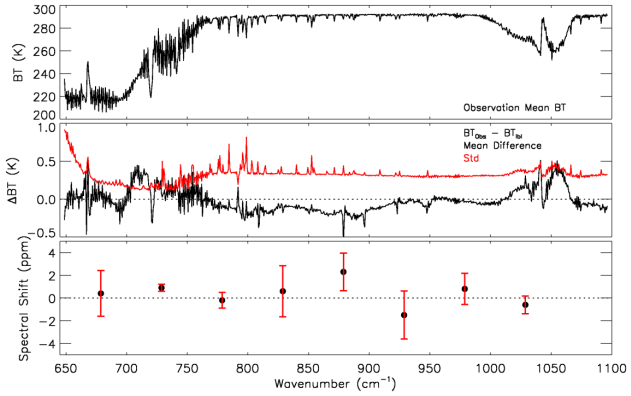

Fig. 4. Spectral shift results using absolute cross-correlation method: between observations and LBLRTM simulations under clear sky over oceans to detect the spectral shift for different spectral ranges (step size 50 cm^{-1}) for FOV 5 at band 1 (LW) for CrIS full resolution unapodized spectra. The mean brightness temperature (BT) for observation (top panel), the mean BT difference between observation and LBL simulation (black line) and standard deviation (red line) (middle panel), and the mean spectral shift (black dot) and standard deviation (vertical bar) at each spectral ranges. The best spectral shift detection regions are: 704-754 cm^{-1} (smallest standard deviation), and 754-804 cm^{-1} (small bias and standard deviation).

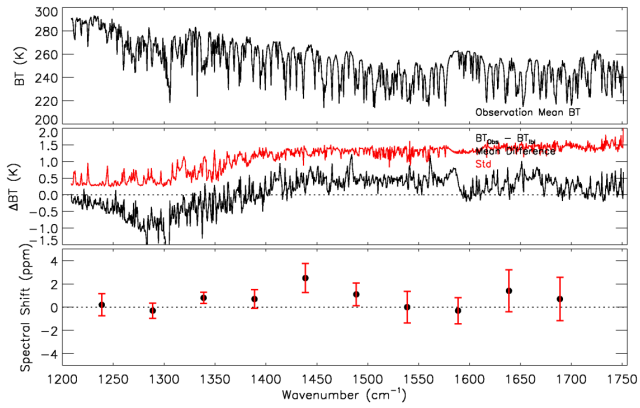

Fig. 5. Same as Fig. 4, except for CrIS band 2 (MW). The best spectral shift detection regions are: 1264-1314 cm^{-1}, and 1314-1364 cm^{-1}.

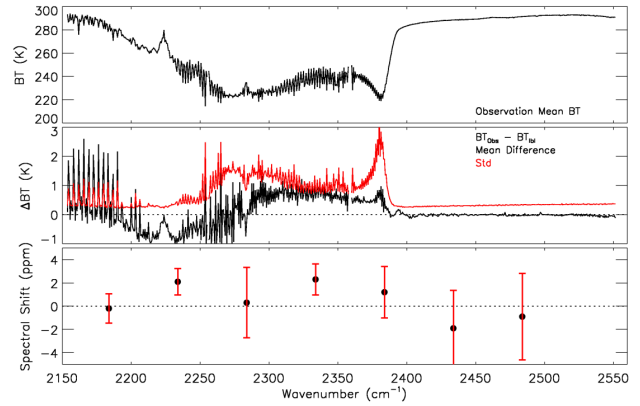

Fig. 6. Same as Fig. 4, except for CrIS band 3 (SW). The best spectral shift detection region is 2160-2210 cm^{-1} at strong CO absorption region. The large mean difference between observations and LBL simulation at this region is due to the default CO profile used in simulation.

LBLRTM. We establish the truth unapodized TOA radiance spectra at the CrIS spectral resolution by performing the following steps: 1) generate line-by-line (LBL) TOA radiance spectra at very fine resolution 0.001 cm^{-1}; 2) convolve them with the CrIS instrument responsivity [Henry Revercomb of University of Wisconsin, personal communication]; 3) transform them by FFT to the interferogram space and truncate them according to CrIS instrument design; 4) and perform inverse FFT to the CrIS spectral resolution and at the same time remove the instrument responsivity.

IV. SPECTRAL REGIONS SELECTION

In order to select the best spectral regions for all three bands, we use the CrIS full spectral resolution SDR data generated offline at NOAA/STAR [15, 22] from February 18 to 20, 2015. We avoid the NSR SDR data because simulations show that the absolute validation of CrIS band 3 was not possible due to the coarse spectral resolution of 2.5 cm^{-1}. Note that in the full spectral resolution SDR processing, the update of the resampling matrix is synchronized with the update of the metrology laser wavelength performed with the Neon measurements roughly once per orbit. The spectral region interval was set to 50 cm^{-1}, in which there are enough gaseous absorption lines for spectral resolution of 0.625 cm^{-1} and have enough frequencies (channels) to apply the cross-correlation method. There are 8, 10, and 7 spectral region intervals, and the starting (ending) wavenumbers are 654 cm^{-1} (1054 cm^{-1}), 1214 cm^{-1} (1714 cm^{-1}), and 2160 cm^{-1} (2510 cm^{-1}) for band 1, band 2, and band 3, respectively. Spectral shift results using the absolute cross-correlation method at FOV 5 for band 1 are shown in Fig. 4. The top panel shows the unapodized mean BT from the observations, and the mean BT difference between observation and LBLRTM simulation (black line) and standard deviation (Std) (red line) are presented at the middle panel. The mean spectral shift (black dot) and standard deviation (vertical bar) at each spectral region are shown at the bottom panel. The absolute BT biases between observations and simulations are within ±0.5 K with these larger biases occurring at CO_2 absorption band (650-750 cm^{-1}) and O_3 band (1020-1070 cm^{-1}). These larger biases mainly come from using the default input profiles for CO_2 and O_3 in the LBLRTM simulations. Except for these CO_2 channels at the beginning of the band and some channels near 790 cm^{-1}, the BT standard deviations are below 0.5 K, while the smallest BT standard deviations are located at 680-760 cm^{-1}. There are two spectral regions standout compared to other spectral regions in terms of absolute spectral shift and standard deviation: 704-754 cm^{-1} (mean: 0.9 ppm; Std: 0.312 ppm), and 754-804 cm^{-1} (mean: -0.2 ppm; Std: 0.693 ppm). Although the spectral region 754-804 cm^{-1} has smallest mean shift, spectral region 704-754 cm^{-1} is selected as the best region in band 1 due to the smallest standard deviation which indicates the spectral shift is very stable and not dependent on the different atmospheric conditions. The absolute shift error can be removed when validating the Neon calibration from the SDR data. The band 2 results are shown in Fig. 5. The absolute BT biases between observations and simulations are at the range of [-1.5 K, 1.0 K], slightly larger than band 1, due to the less accurate water vapor profiles in ECMWF and using default CH_4 profile. Most of the BT standard deviations are around 1.0 K, while the smallest BT standard deviations are located at 1210-1320 cm^{-1} with Std around 0.5 K. The best spectral regions used for detecting spectral shift for band 2 in terms of absolute spectral shift and standard deviation are: 1264-1314 cm^{-1} (mean: -0.3 ppm; Std: 0.657 ppm), and 1314-1364 cm^{-1} (mean: 0.8 ppm; Std: 0.487 ppm). We selected spectral region 1264-1314 cm^{-1} as the best region in band 2 due to the small mean shift and relative small standard deviation and the presence of strong CH_4 absorption lines and water vapor lines. Spectral shift results for band 3 are shown in Fig. 6. The large mean differences between observations and LBLRTM simulations are in the region 2160-2210 cm^{-1}. The spikes in the BT difference and standard deviation in this region are located at the strong CO absorption lines and caused by the inaccurate forward LBLRTM simulation with the default CO profile. However, this region shows the best results for the spectral shift detection with smallest mean shift (-0.2 ppm) and small standard deviation (1.253 ppm). Both quantities are better than

those from CO_2 strong absorption lines located at 2310-2360 cm^{-1} with mean shift 2.3 ppm and standard deviation 1.326 ppm.

The relative spectral validation compared the observed radiances for FOVs 1–4 and 6–9 to the observed radiance for FOV 5. The frequency offset with the maximum correlation coefficient is deemed the spectral shift error relative to the center FOV 5. The relative approach works very well because the inter-FOV validation differences are largely independent of the wavelength region chosen for the cross-correlation process and this approach does not depend on radiances computed from a forward model (such as LBLRTM). It provides the best information on the spectral shifts used to determine the focal plane geometry relative to FOV 5 and works very well for all three bands (LW, MW, and SW) but provides no information regarding absolute validation. However, it does provide an indirect way to check whether the absolute spectral shift value determined from the selected spectral region is good or not. If the chosen spectral region is good, the relative values for the absolute spectral shifts detected using the absolute spectral validation (comparing observed radiances with RT model simulated radiances) from other FOVs compared to that from FOV 5 should be consistent with the relative spectral shift using the relative spectral validation (comparing the observed radiances). Figure 7 shows the absolute spectral shift and relative spectral shift for all CrIS nine FOVs at LW band 1 using spectral range 704-754 cm^{-1}. The spectral shifts relative to FOV 5 agree quite well for these two different techniques if we subtract the FOV 5 shift (0.9 ppm) for the absolute method. In addition to the mean spectral shift consistency, the standard deviations from these shifts for all FOVs are also very consistent. Figures 8 and 9 show the comparison results for band 2 using spectral range 1264-1314 cm^{-1} and band 3 using spectral range 2310-2360 cm^{-1}. The absolute spectral shifts for bands 2 and 3 almost perfectly match with the relative spectral shift considering the small absolute offset at FOV 5. Table II summarizes these spectral offset relative to FOV 5 for both relative and absolute spectral techniques. Note that the absolute results in the parentheses subtract the absolute offset at the FOV 5. For any given FOV, the spectral offsets are almost the same for both methods with maximum differences about 0.1 ppm. These consistent results provide evidence that the absolute validation approach works very well for these chosen spectral regions. The relative spectral validation errors relative to FOV 5 are within 0.5 ppm, 1 ppm, and 1 ppm for LW, MW, and SW bands, respectively. Our study and results from Strow, et al. [11] show that the detector focal plane alignment relative to the interferometer optical axis is extremely stable. Therefore, in the next session we only focus on the long-term spectral accuracy and stability for FOV 5 instead of all FOVs. We also should point out that the absolute spectral validation errors are sensitive to the selection of the particular spectral region. The error in the absolute spectral validation in FOV 5 includes contributions from the region selection, and the Neon calibration error. In fact, Strow, et al. [11] found that there is a calibration error of -0.6 ppm in the Neon calibration for FOV 5. This error is too small to force a change in the Neon calibration, but should be considered in the assessment of the long-term CrIS spectral accuracy and stability.

TABLE II
RELATIVE SPECTRAL DIFFERENCES IN PPM RELATIVE TO FOV 5 FOR ALL THREE BANDS USING FSR SDR DATA[a]

LW			MW			SW		
-0.4 (-0.3)	-0.1 (0)	-0.2 (-0.1)	-0.2 (-0.2)	-0.5 (-0.4)	-1.0 (-1.0)	-0.6 (-0.6)	0 (0.1)	0.1 (0.2)
-0.1 (0)	0	0.1 (0.2)	0.4 (0.4)	0	-0.9 (-0.9)	-0.4 (-0.3)	0	-0.5 (-0.4)
0.2 (0.3)	0.3 (0.4)	0.3 (0.3)	0.7 (0.8)	0.3 (0.3)	-0.2 (-0.2)	0.2 (0.2)	0.4 (0.5)	0.3 (0.4)

[a]The ordering of FOVs 1-9 is from left to right, from up to bottom. These differences are relative to FOV 5 only. Outside of the parentheses are the results using the relative spectral validation method, while inside of the parentheses are the results derived from the absolute spectral validation method by subtracting the FOV 5 absolute spectral shift from the other FOVs. The absolute spectral shifts for FOV 5 are 0.9, -0.3, and -0.2 ppm for LW, MW, and SW, respectively.

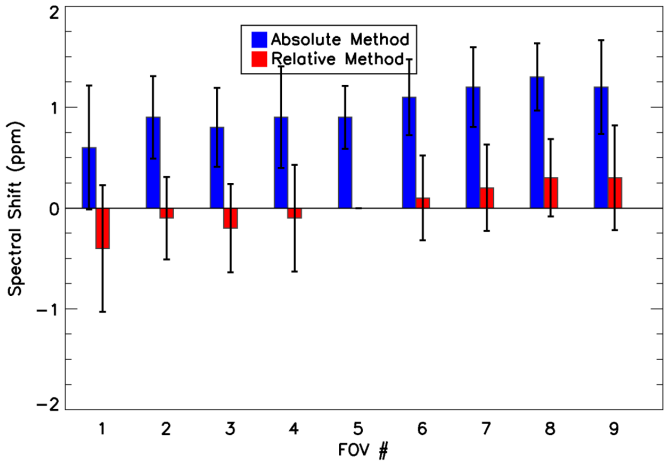

Fig. 7. The absolute spectral shift (LBL V.S. observation) and relative spectral shift (other FOVs V.S. FOV 5) for all CrIS nine FOVs at band 1 spectral range 704-754 cm^{-1}.

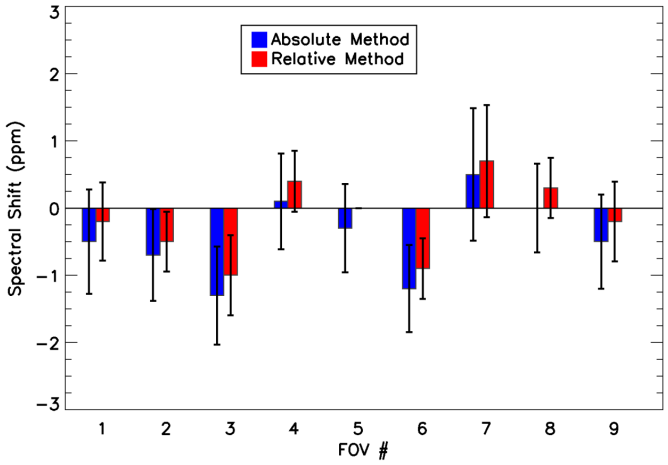

Fig. 8. Same as Fig. 7, except for band 2 spectral range 1264-1314 cm^{-1}.

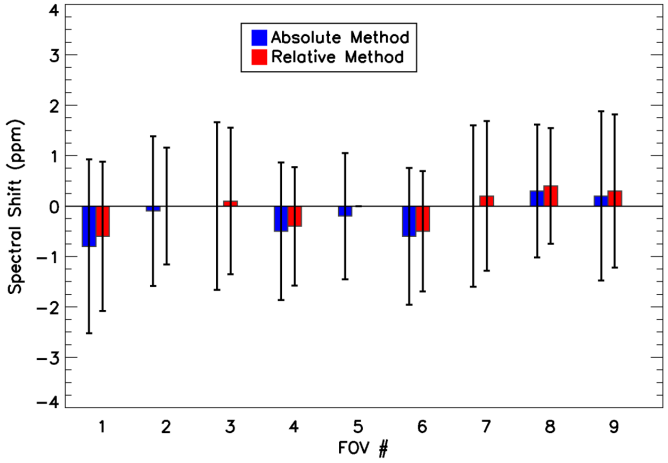

Fig. 9. Same as Fig. 7, except for band 3 spectral range 2160-2210 cm^{-1}.

V. CRIS SDR LONG-TERM SPECTRAL ACCURACY AND STABILITY

The accuracy and stability of the CrIS spectral calibration is examined here using the absolute validation approach discussed in sections III and IV. Nighttime clear uniform ocean tropical scenes for all nine FOVs at the nadir observations (FORs 15 and 16) are detected from the IDPS SDRs by using the cloud detect algorithm coupling CRTM model simulation which uses the spatially and temporally matched ECMWF forecast/analysis as inputs. The simulated spectra are generated using LBLRTM with the same ECMWF forecast/analysis inputs. The computed spectra are cross-correlated with the observed spectra using the three steps described in section III. The spectral offset that produces the maximum correlation coefficient between the computed and observed spectra is the absolute spectral error of the observed spectra. The absolute spectral error is averaged daily among these clear scenes since the metrology laser wavelength is relative stable and we do not expect large variation during a day (except for sharp spikes and during CMO update periods). Figure 10 shows the daily averaged absolute spectral validation error derived from band 1 (blue line with open circle) using the IDPS SDR data from September 22, 2012 to April 19, 2016. This curve has been offset by 0.6 ppm (instead of 0.9 ppm indicated by the results from Section IV) in order to agree with the Neon calibration. The red curve is the relative variation of the metrology laser wavelength as measured by the Neon calibration subsystem. The relative variation of the metrology laser wavelength is defined as

$$\Delta\nu_L(\text{ppm}) = \frac{(\nu_R - \nu)*10^6}{\nu_R}, \tag{8}$$

where ν_R is the reference wavelength, and is set to 1546.26096 nm which is the metrology laser wavelength on December 19, 2012 at 7:42:12. At that time, the CMO in the IDPS was updated due to the occurrence of a sharp spike, and the resampling wavelength was set to the metrology laser wavelength. The black curve is the daily averaged sampling error computed using (4), which is the relative difference between the Neon measured laser wavelength and the resampling wavelength used in the frequency calculation for the spectra on the sensor grid. The sampling error before February 20, 2014 is not included in the figure because the resampling wavelength was not recorded correctly as mentioned early. Note that the relative variation of the metrology laser wavelength is plotted every 8 seconds (for each scan), while the sampling error and the absolute spectral error are daily averages. The vertical dashed line in this figure is same as that in Fig. 2, indicating the time of EP version 36 uploading and IDPS software fixing the ILS equation error for FOV 5.

The absolute spectral validation error detected from the absolute method between observations and LBLRTM simulations includes several possible error sources: the software issues about the sampling interval using in the resampling matrix and ILS equation error for FOV 5; the CrIS Neon calibration subsystem (especially the effective Neon wavelength) stability issue during the mission; the sampling error in the processing system; the spectral correction of SA effects based on the ILS parameters; and the error from the cross-correlation method itself such as the dependence on the selection of spectral regions showed in section IV, which can be treated as a systemic error and easily removed by a constant offset. The results showed in Fig. 10 give very complicated and mixed patterns. It is not easy and straight-forward to explain the features of the absolute spectral error. First, the relative variation of the metrology laser wavelength has a period of about one year (primarily due to the temperature changes in the interferometer baseplate) and is relatively stable. However, we do see a negative slope trending occurring in the last cycle which may indicate changes of the effective Neon wavelength in the CrIS Neon calibration subsystem. Second, as explained in Fig. 2, before November 14, 2013, the resampling wavelength is incorrect in the SDR data. After the fix, it still changes too frequently, and does not follow the software design in which the resampling wavelength changes only after the cumulative variation of the

metrology laser wavelength exceeding 2 ppm. Third, there are two occurrences for the absolute spectral error changing about 2 ppm: the first one is on November 14, 2013, where the IDPS software was updated to fix the resampling wavelength which is saved to the CMO file; the second one is on February 20, 2014, where the IDPS software was updated to fix the ILS equation error for FOV 5. In both cases, the CMO is recomputed, and the resampling wavelength is set to the metrology laser wavelength resulting in the absolute spectral error around zero. The absolute spectra error immediately after the first jump is not near zero is just because of the 1.4 ppm spectral shift caused by the ILS equation error for band 1 at FOV 5 before February 20, 2014. Instead of following metrology laser wavelength with peak to peak 3 ppm shift, the actual spectral error from the operational SDRs generated by the IDPS software and determined by the absolute spectral validation method is about 4 ppm from peak to peak during the CrIS mission, and follows the sampling error very closely after February 20, 2014.

In order to clearly understand the possible spectral error sources, and thoroughly evaluate the spectral accuracy and stability from the operational SDR data during the CrIS mission, we divide the mission into two time slots, before and after February 20, 2014. Figure 11 shows the comparison results of the metrology laser wavelength variation measured with the Neon calibration subsystem versus spectral calibration error of the IDPS spectra assessed using RT model from September 22, 2012 to February 19, 2014 before the EP version 36 update. The spectral error using RT model for band 1 from the IDPS SDRs are offset by 1.4 ppm due to bugs in the IDPS SDR software without considering the FOV5 geometry offset in the detector when applying SA correction. During this period, we only know CMO recomputed three times (there may have one on April 17, 2013) in the IDPS SDRs processing, December 19, 2012 at 7:42:12, July 10, 2013 at 15:05:37, and November 14, 2013 at 18:43:22 (These times are indicated by the vertical dashed lines in this figure). From December 17, 2012 to April 17, 2013, the spectral error using RT model is almost perfectly follows the relative spectral variation from the Neon calibration subsystem, which indicates that the error source is primarily dominated by the sampling error in the SDR data and results from the metrology laser wavelength continuously drifts while the resampling wavelength was kept the same. From April 17, 2013 to July 10, 2013, a slight departure (less than 0.3 ppm) between the spectral error and the relative spectral variation of the metrology laser wavelength is found. This slight departure indicates that there may have a recomputed CMO around this period, in which the resampling wavelength was updated with the metrology laser wavelength. During this period, the relative spectral variation from metrology laser wavelength is around zero and absolute spectral error is also small. From July 10, 2013 to November 14, 2013, the absolute spectral error using RT model is perfectly aligning again with the relative spectral variation from the Neon calibration subsystem. During this period, the absolute spectral variation of the metrology laser wavelength is about 2 ppm. After the CMO recomputed with the updated resampling wavelength (which is equal to half of metrology laser wavelength, and resulting in zero sampling error) on November 14, 2013, the absolute spectral error using RT model is near zero, and is departed by about 2 ppm from the relative spectral variation calculated from the Neon calibration subsystem after that day. The near constant spectral shift departure between RT model and Neon calibration subsystem after that day is exactly what we expect from the IDPS SDR data, which is followed the original spectral calibration design in the software that the resampling wavelength keeps the same and this departure represents the sampling error in the data.

There are two ways to remove the sampling error in the SDR data: 1) CMO update daily (metrology laser wavelength changes in a day can be negligible) and processing the SDR daily; 2) using the updated metrology laser wavelength as the resampling wavelength length (see (1)) to compute the resampling matrix, but keeping the same for the SA matrix calculation based on the fact the SA matrix does not dependent on the resampling wavelength change assuming the laser wavelength variation is less than 100 ppm for the whole CrIS mission. It is relatively easy to carry out for the first approach. However, for the second approach, the processing software has to update accordingly. The CMO has to separate into two parts, one static part including the reverse SA matrix, and one dynamic part including resampling matrix. The CMO matrix is dynamically generated by combining inverse matrix with the resampling matrix and post filter. To improve the spectral calibration accuracy and increase the data consistency, we did both ways. The results using the reprocessed SDRs generated by ADL for the first approach are shown in Fig. 11. The reprocessed SDRs with CMO update daily are using latest updated non-linearity coefficients and ILS parameters in Engineering Packet version 36 and from May 1, 2013 to September 26, 2013. The validation error using RT model for band 1 (green line with triangle symbol) and band 2 (yellow line with square symbol) are near zero (after offset the biases of -0.6 ppm and 0.3 ppm for band 1 and band 2, respectively) during this period. Note that the band 2 spectral validation error agrees very well with the band 1 validation error although it has larger variation from day to day. It is clear that the first approach can effectively remove the sampling error inherited from the SDR data, which were generated with the resampling wavelength instead of the metrology laser wavelength to calculate the sensor grid resolution in (1) and use in the CMO computation. However, this approach is not convenient for users to reprocess the SDR data since users have to process the data day by day.

The second approach is implemented in CrIS full spectral resolution processing system FSR-ADL which is used to generate the CrIS FSR SDRs and available for the user community after S-NPP CrIS commanded to the FSR mode from the NSR mode on December 4, 2014. These offline generated FSR SDRs can be important independent data sources to check the CrIS absolute and relative spectral

calibration accuracy when comparing the results from the operational IDPS SDRs. Figure 12 shows the spectral validation results after February 20, 2014 when the IDPS software bugs are fixed for the FOV 5 ILS equation error and resampling wavelength is recorded in the CMO files. The red line is the difference between the absolute spectral error assessed using RT model of band 1 (blue line with open circle in Fig. 10) and the sampling error computed using (4) (black line in Fig. 10). This spectral error difference has a slight negative trend during this period. It is clear that this spectral error difference is around -0.2 to -0.3 ppm after November 2014 from the IDPS SDR data. This feature is independently verified by the CrIS FSR data. The CrIS three bands spectral error results using RT model from the CrIS FSR data are superimposed on this graph. The green line with triangle symbol is the daily averaged spectral error using RT model for band 1. This curve has been offset by 0.6 ppm in order to consistently agree with results from the Neon calibration subsystem and the reprocessed NSR SDRs data at Fig. 11. The band 1 spectral error derived from the FSR SDR data tracks the spectral error difference between the spectral error using RT model from the IDPS NSR band 1 and the sampling error quite accurately. As shown in section IV, the absolute spectral error for band 1 using the FSR SDRs is about -0.9 ppm (the negative sign indicates observations relative to LBL results). This -0.3 ppm spectral error observed by the FSR SDR data and the IDPS NSR SDR data may indicate that the effective Neon wavelength changes in the CrIS Neon calibration subsystem. Unfortunately, we could not derived the same spectral error and negative trending using RT model from bands 2 and band 3 for the FSR SDR data due to the larger variation of the daily averaged shift although they in general agree with well each other and following the trending.

Another way to check the spectral accuracy and stability for the IDPS NSR SDR data after December 4, 2014 is to use the relative spectral validation method with the offline generated FSR SDR data. Since the band 1 in both the NSR and the FSR SDR data has same spectral resolution, it is relatively easy to apply the relative spectral validation method for these two SDR datasets. Figure 13 shows the band 1 daily averaged spectral error between the NSR SDR and the FSR SDR using the relative spectral validation method (red line), the sampling error (black line as shown in Fig. 10), and absolute spectral error using RT model for the NSR (blue line as shown in Fig. 10) and the FSR SDR data (green line with triangle symbol as shown in Fig. 12). Note that the daily relative spectral error difference between the NSR and the FSR SDR data using RT model is also shown in here (cyan blue) which is aligning very well with the red line. The red line almost perfectly tracks the black line, which indicates that the resampling wavelength is correctly recorded in the CMO files and used in the IDPS NSR SDR data, although it is not following the original design to change only after the cumulative variation of the metrology

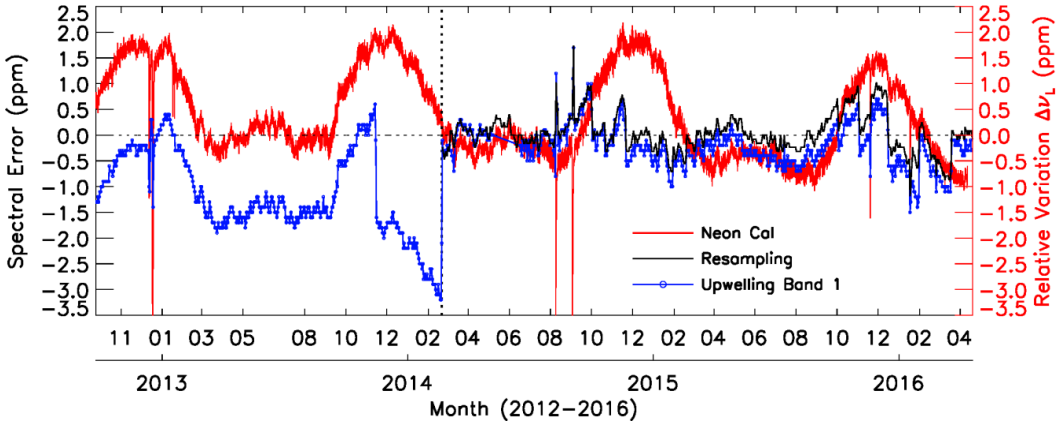

Fig. 10. Comparison of the Neon calibration subsystem (red line, indicated by "Neon Cal") versus validation using RT model (bule line with open circle, indicated by "Upwelling Band 1") for the IDPS SDRs from September 22, 2012 to April 19, 2016. The absolute spectral error using RT model is for the daily average of FOV5 at nadir (FORs 15 or 16), descending orbit over clear tropical ocean scenes. The sampling error (black line, indicated by "Resampling") due to using the resampling wavelength (used in the IDPS to calculate the correction matrices) instead of the metrology laser wavelength after February 20, 2014 is also shown. The vertical dashed line is the same as in Fig. 2. Note that the data from the absolute spectral error using RT model are missing in the period from May 8, 2014 to June 16, 2014 due to loss of ECMWF model forecast files.

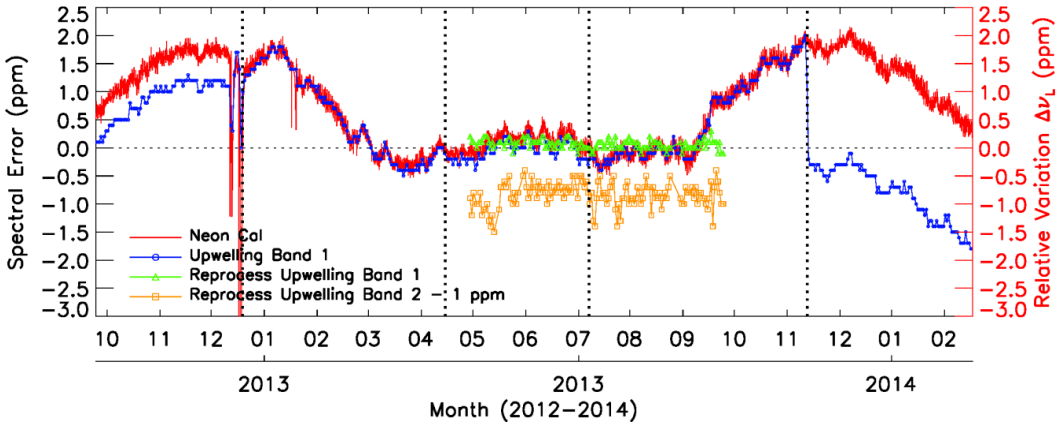

Fig. 11. Comparison of the Neon calibration subsystem versus validation using RT model for the IDPS SDRs from September 22, 2012 to February 19, 2014 before the Engineering Packet version 36 update. The spectral error using RT model for band 1 from the IDPS SDRs is offset by 1.4 ppm (see text). The spectral error using RT model for bands 1 and 2 from the reprocessed SDRs generated by ADL are near zero (after offset the biases of -0.6 ppm and 0.3 ppm for band 1 and band 2, respectively). The reprocessed SDRs with CMO update daily are using updated non-linearity coefficients and ILS parameters in Engineering Packet version 36 and from May 1, 2013 to September 26, 2013. The four vertical dashed lines are for CMO update times: December 19, 2012, April 17, 2013 (probably), July 10, 2013, and November 14, 2013.

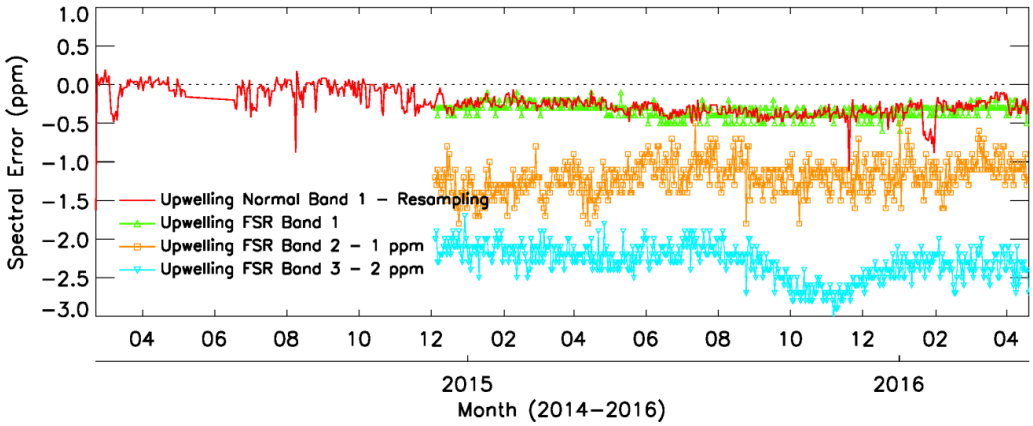

Fig. 12. The spectral validation results from February 20, 2014 to April 19, 2016. The red line is the averaged daily spectral error difference between the spectral error for band 1 using RT model (blue line with open circle in Fig. 10) and the sampling error (black line in Fig. 10). The CrIS three bands spectral error results using RT model from CrIS FSR data are superimposed on this graph. The green line with triangle symbol is for band 1 results (offset by -0.6 ppm in order to consistently agree with results from Neon calibration subsystem and the reprocessed NSR SDRs data at Fig. 11). Note that the absolute spectral error data are missing in the period from May 8, 2014 to June 16, 2014 due to loss of ECMWF model forecast files.

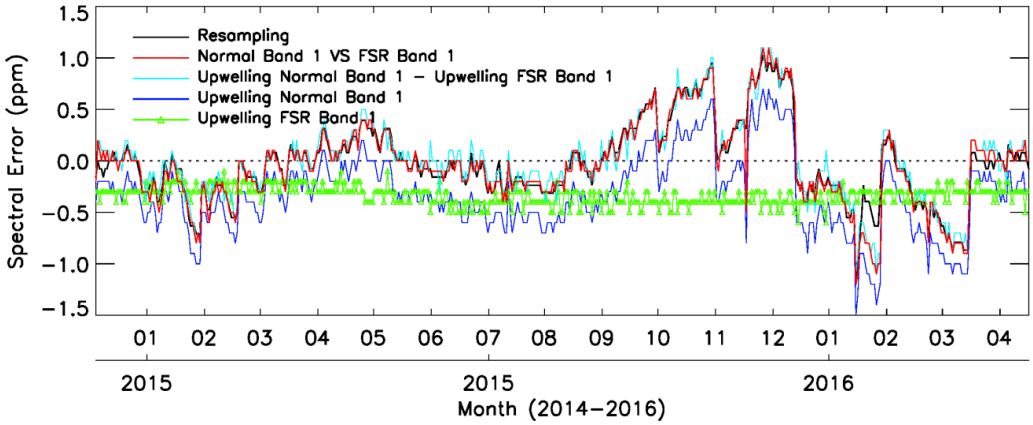

Fig. 13. The band 1 daily averaged spectral error between the NSR SDR and the FSR SDR using the relative spectral validation method (red line), the sampling error (black line as shown in Fig. 10), and spectral error using RT model for the NSR (blue line as shown in Fig. 10) and the FSR SDR data (green line with triangle symbol as shown in Fig. 12). Note that the daily spectral error difference between the NSR and the FSR SDR data using RT model is also shown in here (cyan blue) which is aligning very well with the red line. The period is from December 4, 2014 to April 19, 2016.

laser wavelength exceeding 2 ppm. If the effective Neon wavelength in the Neon calibration subsystem is perfect and stable, two features will be observed in the spectral error: 1) the absolute spectral error using RT model for NSR SDR (blue line) will follow the sampling error (black line); 2) the absolute spectral error using RT model for FSR SDR (green

line) will be zero since we always use the metrology laser wavelength to calculate the sensor grid resolution. Both 1) and 2) do not occur as shown in Figs. 12 and 13. There are discrepancies from black line and blue line, and green line is not near zero but around -0.3 ppm. These two evidences indicate that the effective Neon wavelength in Neon calibration subsystem may be changed slightly after November 2014. The root cause for the negative trending of effective Neon wavelength change is unknown at the point, which warrants a close monitoring for any further changes.

As shown in this study, the operational IDPS SDR data have around 4 ppm peak-to-peak spectral calibration errors during the S-NPP mission life time. From NWP data assimilation and weather forecast and deriving climate trend perspectives, the radiometric errors due to spectral calibration error could be negligible for CrIS apodized spectra, but have to take the spectral shift into account for the unapodized spectra due to the larger BT impact for the temperature sounding channels located at 650 cm^{-1} to 770 cm^{-1} and the whole water vapor channels in band 2 (see Fig. 1). To reduce the radiometric errors due to the spectral calibration errors and derive climate trending such as CO_2 concentration, temperature, and water vapor from the CrIS SDR data, it is very necessary and critical to reprocess the whole S-NPP mission SDR data to remove these spectral shifts in the operational SDR data using the method we proposed in this study, in which the CMO is separated into the unchanged reverse SA matrix and the resampling matrix using the metrology laser wavelength from the Neon calibration subsystem as resampling wavelength.

VI. SUMMARY AND CONCLUSION

Since the launch of S-NPP satellite, CrIS has provided more than four years of measurements. In this study, the long-term spectral calibration accuracy and stability are evaluated using CrIS operational SDR data generated by the IDPS. Two spectral validation methods are presented using maximum cross-correlation techniques: relative and absolute methods. These spectral validation methods are applied to the tropical ocean clear uniform scenes. The CrIS clear scenes are detected using the brightness temperature departure between the CRTM model simulations and observations. The best spectral regions are selected based on the spectral shift determined from the absolute method between observations and LBLTM simulations. With small bias and small standard deviation as the spectral shift requirements, three spectral regions 704-754 cm^{-1}, 1264-1314 cm^{-1}, and 2160-2210 cm^{-1} using the CrIS full spectral resolution SDR are selected for CrIS three bands, respectively. The relative spectral offsets for FOVs 1-4 and 6-9 relative to FOV 5 with both relative and absolute spectral techniques are within 1ppm, which indicates that the ILS parameters for the nine focal plane relative positions are well determined. In addition, for any given FOV relative to FOV 5, the spectral offsets are almost the same for both methods with maximum different at 0.1 ppm. These consistent results provide evidence that the absolute validation approach works very well for these chosen spectral regions. Based on these results, these selected spectral ranges can be used to evaluate the spectral accuracy and stability for CrIS, IASI and future FTS infrared instruments. For these FTS infrared instruments without hardware calibration subsystem, the method presented in this study provides a very reliable way to assess the long-term spectral stability and trending.

CrIS has experienced less than 3 ppm peak to peak annual variation in the metrology laser wavelength as measured by the Neon calibration subsystem during the mission. The current operational algorithm was designed to have a spectral calibration to be better than 2 ppm, however, due to the IDPS software bugs (such as not saving the resampling laser wavelength in CMO files, and the FOV 5 ILS equation error) the spectral calibration errors in the SDR data have shown about 4 ppm peak to peak variations during the period from September 22, 2012 to April 19, 2016. The spectral shift errors in the operational SDRs were not following the sampling error related to the metrology laser wavelength especially before July 10, 2013, and occasionally jumped up and down when a new CMO was computed due to the ILS parameters changes or software updates, thus resulted in a very poor spectral stability. Since the radiometric accuracy depends upon accurate spectral calibration, it is very important to reduce the CrIS spectral uncertainty and increase the stability for weather and climate applications. Two ways to increase the CrIS spectral calibration stability were considered: 1) the CMO is updated daily, and 2) the CMO is separated into the unchanged reverse SA matrix and the resampling matrix using the updated metrology laser wavelength from the Neon calibration subsystem as the resampling wavelength. Using these two methods, the spectral calibration stability in the CrIS SDR can be significantly improved to within 0.5 ppm as shown in the reprocessed NSR and offline FSR SDRs data. Using the reprocessed NSR SDRs with daily recomputed CMO during period from May 1, 2013 to September 26, 2013 and the CrIS FSR data with the new CMO correction method after December 4, 2014 as two independent data sources, the absolute spectral error is found that for band 1 FOV 5 is about negative 0.6 ppm, which is consistent with the results from Strow, et al. [11]. A negative trending is found in the spectral calibration error during CrIS mission. There is about -0.3 ppm spectral calibration error in the FSR SDR data and the IDPS NSR SDR data after December 4, 2014, and it may indicate that the effective Neon wavelength changes in the CrIS Neon calibration subsystem. However, the root cause for the negative trending of effective Neon wavelength change is unknown at the point, which warrants a close monitoring for any further changes.

REFERENCES

[1] J. Le Marshall, J. Jung, J. Derber, M. Chahine, R. Treadon, S. J. Lord*, et al.*, "Improving global analysis and forecasting with AIRS," *Bulletin of the American Meteorological Society,* vol. 87, pp. 891-894, Jul 2006.

[2] F. Hilton, R. Armante, T. August, C. Barnet, A. Bouchard, C. Camy-Peyret*, et al.*, "HYPERSPECTRAL EARTH

OBSERVATION FROM IASI Five Years of Accomplishments," *Bulletin of the American Meteorological Society,* vol. 93, pp. 347-+, Mar 2012.

[3] D. Liang, F. Z. Weng, and Ieee, "EVALUATION OF THE IMPACT OF A NEW QUALITY CONTROL METHOD ON ASSIMILATION OF CRIS DATA IN HWRF-GSI," in *2014 Ieee International Geoscience and Remote Sensing Symposium*, ed New York: Ieee, 2014, pp. 3778-3781.

[4] N. Smith, W. L. Smith, E. Weisz, and H. E. Revercomb, "AIRS, IASI, and CrIS Retrieval Records at Climate Scales: An Investigation into the Propagation of Systematic Uncertainty," *Journal of Applied Meteorology and Climatology,* vol. 54, pp. 1465-1481, Jul 2015.

[5] H. H. Aumann and T. S. Pagano, "Using AIRS and IASI data to evaluate absolute radiometric accuracy and stability for climate applications," in *Atmospheric and Environmental Remote Sensing Data Processing and Utilization Iv: Readiness for Geoss Ii*. vol. 7085, M. D. Goldberg, H. J. Bloom, P. E. Ardanuy, and A. H. L. Huang, Eds., ed, 2008.

[6] M. Goldberg, G. Ohring, J. Butler, C. Cao, R. Datla, D. Doelling*, et al.*, "THE GLOBAL SPACE-BASED INTER-CALIBRATION SYSTEM," *Bulletin of the American Meteorological Society,* vol. 92, pp. 467-475, Apr 2011.

[7] L. Wang, Y. Han, X. Jin, Y. Chen, and D. A. Tremblay, "Radiometric consistency assessment of hyperspectral infrared sounders," *Atmospheric Measurement Techniques,* vol. 8, pp. 4831-4844, 2015 2015.

[8] L. Wang and C. Cao, "On-Orbit Calibration Assessment of AVHRR Longwave Channels on MetOp-A Using IASI," *Ieee Transactions on Geoscience and Remote Sensing,* vol. 46, pp. 4005-4013, Dec 2008.

[9] Y. Han, H. Revercomb, M. Cromp, D. G. Gu, D. Johnson, D. Mooney*, et al.*, "Suomi NPP CrIS measurements, sensor data record algorithm, calibration and validation activities, and record data quality," *Journal of Geophysical Research-Atmospheres,* vol. 118, pp. 12734-12748, Nov 27 2013.

[10] D. Tobin, H. Revercomb, R. Knuteson, J. Taylor, F. Best, L. Borg*, et al.*, "Suomi-NPP CrIS radiometric calibration uncertainty," *Journal of Geophysical Research: Atmospheres,* vol. 118, pp. 10,589-10,600, 2013.

[11] L. L. Strow, H. Motteler, D. Tobin, H. Revercomb, S. Hannon, H. Buijs*, et al.*, "Spectral calibration and validation of the Cross-track Infrared Sounder on the Suomi NPP satellite," *Journal of Geophysical Research-Atmospheres,* vol. 118, pp. 12486-12496, Nov 27 2013.

[12] L. Wang, D. A. Tremblay, Y. Han, M. Esplin, D. E. Hagan, J. Predina*, et al.*, "Geolocation assessment for CrIS sensor data records," *Journal of Geophysical Research-Atmospheres,* vol. 118, pp. 12690-12704, Nov 27 2013.

[13] V. Zavyalov, M. Esplin, D. Scott, B. Esplin, G. Bingham, E. Hoffman*, et al.*, "Noise performance of the CrIS instrument," *Journal of Geophysical Research-Atmospheres,* vol. 118, pp. 13108-13120, Dec 2013.

[14] Y. Chen, Y. Han, and F. Z. Weng, "Detection of Earth-rotation Doppler shift from Suomi National Polar-Orbiting Partnership Cross-Track Infrared Sounder," *Applied Optics,* vol. 52, pp. 6250-6257, Sep 2013.

[15] Y. Chen, Y. Han, D. Tremblay, L. Wang, X. Jin, and F. Weng, "CrIS full resolution processing and validation system for JPSS," presented at the the 19th International TOVS Study Conference (ITSC-19), Jeju Island, South Korea, 2014.

[16] A. P. McNally and P. D. Watts, "A cloud detection algorithm for high-spectral-resolution infrared sounders," *Quarterly Journal of the Royal Meteorological Society,* vol. 129, pp. 3411-3423, Oct 2003.

[17] Y. Chen, F. Z. Weng, Y. Han, and Q. H. Liu, "Validation of the community radiative transfer model by using CloudSat data," *Journal of Geophysical Research-Atmospheres,* vol. 113, Jul 25 2008.

[18] Y. Chen, Y. Han, P. Van Delst, and F. Z. Weng, "On water vapor Jacobian in fast radiative transfer model," *Journal of Geophysical Research-Atmospheres,* vol. 115, Jun 19 2010.

[19] Y. Chen, Y. Han, P. van Delst, and F. Z. Weng, "Assessment of Shortwave Infrared Sea Surface Reflection and Nonlocal Thermodynamic Equilibrium Effects in the Community Radiative Transfer Model Using IASI Data," *Journal of Atmospheric and Oceanic Technology,* vol. 30, pp. 2152-2160, Sep 2013.

[20] C. Y. Cao, J. Xiong, S. Blonski, Q. H. Liu, S. Uprety, X. Shao*, et al.*, "Suomi NPP VIIRS sensor data record verification, validation, and long-term performance monitoring," *Journal of Geophysical Research-Atmospheres,* vol. 118, p. 15, Oct 2013.

[21] S. A. Clough, M. W. Shephard, E. Mlawer, J. S. Delamere, M. Iacono, K. Cady-Pereira*, et al.*, "Atmospheric radiative transfer modeling: a summary of the AER codes," *Journal of Quantitative Spectroscopy & Radiative Transfer,* vol. 91, pp. 233-244, Mar 1 2005.

[22] Y. Han, Y. Chen, X. Xiong, and X. Jin, "S-NPP CrIS full resolution SDR processing and data quality assessment," presented at the the 95th AMS Annual Meeting, Phoenix, Arizona, 2015.

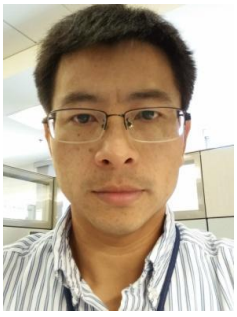

Yong Chen received the B.S. and M.S. degree in atmospheric sciences from Peking University, Beijing, China, in 1996 and 1999, respectively, and the Ph.D. degree in atmospheric sciences from University of California, Los Angeles, in 2006.

From 2006 to 2013, he was a research scientist with the Cooperative Institute for Research in the Atmosphere, Colorado State University. From 2013 to present, he is a research scientist with Earth System Science Interdisciplinary Research Center, University of Maryland at

College Park. The major fields that he is working on include the following: 1) Radiative transfer theory and applications; 2) Development and implementation of fast radiative transfer model for satellite data assimilation; 3) Radiometric and spectral calibration and validation of satellite hyper-spectral infrared sounder.

Yong Han received his B.S. and M.S. degrees in 1982 and 1985, respectively, from the Nanjing Institute of Meteorology, Nanjing, China, in atmospheric science, and the Ph.D. degree in meteorology from the Pennsylvania State University, University Park, in 1992.

He was a postdoctoral research associate with the National Research Council from 1992 to 1994, a physical scientist with the University of Colorado/Cooperative Institute for Research in the Environmental Sciences/NOAA Environmental Technology Laboratory from 1994 to 2001, and a research scientist at the Science Systems and Applications, Inc./NASA Goddard Space Flight Center, Greenbelt, MD, in 2002. During these periods his research activities included microwave and infrared radiometer calibrations, radiative transfer modeling, development of retrieval algorithms and ground-based atmospheric remote sensing. Since 2002, he has been a physical scientist at the Center for Satellite Applications and Research (STAR) of the NOAA National Environmental Satellite, Data and Information Service (NESDIS), working on various research projects, including those supported by the Joint Center for Satellite Data Assimilation (JCSDA) and the Joint Polar Satellite System (JPSS) program. His research interests include radiometric instrument calibration and validation, radiative transfer modeling, mathematical retrieval methods and atmospheric remote sensing.

Fuzhong Weng received his Ph.D. degree in 1992 from Department of Atmospheric Science, Colorado State University (CSU), Fort Collins, USA.

He is the chief of Satellite Meteorology and Climatology of NOAA/NESDIS/Center for Satellite Applications and Research, Senior Scientist of Joint Center for Satellite Data Assimilation (JCSDA), and JPSS Sensor Science Chair. He won a number of awards including the first winner of the 2000 NOAA David Johnson Award for his outstanding contributions to satellite microwave remote sensing fields and the utilization of satellite data in the NWP models, US Department of Commerce Gold Medal Award in 2005 for his achievement in satellite data assimilation, NOAA bronze medal for leading successful NOAA-18 instrument calibration, and NOAA Administrator's Award for developing new and powerful radiative transfer models to assimilate advanced satellite data in 2009 and NOAA Administrator's Award for leadership in developing a state-of-the art satellite instrument health monitoring system enabling corrective actions to extend instrument life. He has published over 160 papers in American journals (e.g AMS, AGU, IEEE) and other international journals.